DEPARTMENT OF MECHANICAL ENGINEERING AND MECHANICS
SCHOOL OF ENGINEERING
OLD DOMINION UNIVERSITY
NORFOLK, VIRGINIA

IMPACT DAMAGE OF COMPOSITE PLATES

By

K. M. Lal, Co-Principal Investigator

and

G. L. Goglia, Principal Investigator

Progress Report
For the period September 1982 to March 1983

Prepared for the
National Aeronautics and Space Administration
Langley Research Center
Hampton, Virginia

Under
Research Grant NAG1-196
Walter Illg, Technical Monitor
Materials Division

April 1983

OLD DOMINION UNIVERSITY RESEARCH FOUNDATION

DEPARTMENT OF MECHANICAL ENGINEERING AND MECHANICS
SCHOOL OF ENGINEERING
OLD DOMINION UNIVERSITY
NORFOLK, VIRGINIA

IMPACT DAMAGE OF COMPOSITE PLATES

By

K. M. Lal, Co-Principal Investigator

and

G. L. Goglia, Principal Investigator

Progress Report
For the period September 1982 to March 1983

Prepared for the
National Aeronautics and Space Administration
Langley Research Center
Hampton, Virginia

Under
Research Grant NAG1-196
Walter Illg, Technical Monitor
Materials Division

Submitted by the
Old Dominion University Research Foundation
P.O. Box 6369
Norfolk, Virginia 23508

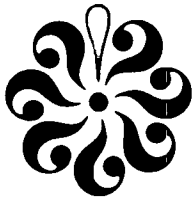

April 1983

IMPACT DAMAGE OF COMPOSITE PLATES

By

K.M. Lal[1] and G.L. Goglia[2]

SUMMARY

During the first half of the current year (September 1982 to March 1983) the following work was done:

1. Development of a model for coefficient of restitution.

This model is based on idealized shear dominated theory of fiber-reinforced composite laminates which assumes that the fibers are inextensible in fiber direction and that the fibers are incompressible in in z-direction. This model is strictly limited to thin plates of quasi-isotropic composite material.

Predictions were compared with the test results for circular and rectangular plates of various sizes. The similarity between theory and experiment was found better than could reasonably be expected, in view of the very simple nature of the theory.

A manuscript "Coefficient of restitution for low velocity transverse impact of thin graphite-epoxy laminates" (Appendix A) describes the model, and is enclosed herewith.

2. The experience of impact tests in the laboratory revealed that the variation of force and central deflection during an impact event could be represented by half-sine waves, with a phase lag between force and deflection. An attempt was made to correlate the phase difference with the energy absorbed by the target. Since the energy absorbed by the target is equal to the energy lost by the impactor during impact, which can be easily calculated by incorporating the coefficient of restitution, a model was developed to correlate the coefficient of restitution with the phase difference between force and deflection.

[1] Associate Research Professor, Department of Mechanical Engineering and Mechanics, Old Dominion University, Norfolk, Virginia 23508.
[2] Eminent Professor/Chairman, Department of Mechanical Engineering and Mechanics, Old Dominion University, Norfolk, Virginia 23508.

Comparison of the predictions with the experimental test results was very encouraging.

A manuscript "Relationship between phase difference and coefficient of restitution during low velocity foreign objects transverse damage of composite plates" (Appendix B) is enclosed.

3. Work to evaluate the state of stress in various plies surrounding the point of impact is in process. Report is expected to come in about 3 to 4 months.

APPENDIX A

COEFFICIENT OF RESTITUTION FOR LOW VELOCITY TRANSVERSE IMPACT OF THIN GRAPHITE-EPOXY LAMINATES

K. M. Lal*
NASA Langley Research Center
Hampton, Virginia

ABSTRACT

This paper discusses a simple model to study low velocity transverse impact of thin plates made of fiber-reinforced composite material, in particular T300/5208 graphite-epoxy. This model predicts the coefficient of restitution, which is a measure of the energy absorbed by the target during an impact event. The model is constructed on the assumption that the plate is inextensible in the fiber direction and that the material is incompressible in the z-direction. Such a plate essentially deforms by shear, hence this model neglects bending deformations of the plate. The coefficient of restitution is predicted to increase with large interlaminar shear strength and low transverse shear modulus of the laminate.

Predictions are compared with the test results of impacted circular and rectangular clamped plates. Experimentally measured values of the coefficient of restitution are found to agree with the predicted values within a reasonable error.

INTRODUCTION

During the last decade, the advanced graphite-epoxy composite materials have offered specific strength and modulus properties superior to those of conventional monolithic materials. These advanced composites have potential

*Also, Research Associate Professor of Mechanical Engineering and Mechanics at Old Dominion University, Norfolk, Virginia.

for use in aerospace structures, but they appear to be susceptible to transverse impact damage. The problem of determining the energy absorbed by the target is of interest, because this energy can reduce the integrity of the target.

The energy absorbed by the target during an impact event is equal to the loss in kinetic energy of the impactor. Mathematically, the energy lost, I_a, by an impactor during the impact process is given by

$$I_a = I(1 - e^2) \tag{1}$$

where I is the maximum amount kinetic energy carried by the impactor and e is the coefficient of restitution. Thus, the coefficient of restitution is a measure of the energy lost by the impactor and is equal to the ratio of the velocity at the time of rebound to the maximum velocity of the impact. Because the coefficient of restitution is needed to compute the absorbed energy, the objective of this work is to develop a mathematical model of the coefficient of restitution of thin anisotropic plates.

ANALYSIS

Composite plates are laid up by laminating thin sheets of unidirectionally reinforced material. Macroscopically the fibers may be regarded as continuously distributed through the plate and the material is transversely isotropic about the axis normal to the plate. For graphite-epoxy composites, $E_f >> E_m$, i.e., the fiber is very much stiffer than the matrix. The resistance of a lamina to extension in the fiber direction may be several orders of magnitude greater

than its resistance to transverse extension or transverse shear. This property can be idealized by assuming that all laminae are inextensible in the fiber direction [1]. For mathematical convenience, it will also be assumed that the composite is incompressible in transverse direction. This assumption is frequently made in solid mechanics.

Consider a plate having its middle surface lying in the plane $z = 0$. The fibers are in the planes z = constant and are arranged in families having multidirections. If ϕ is the angle between the x-axis and a particular family of fibers, the condition for inextensibility in the fiber direction is given by [2],

$$\varepsilon_1 = \frac{\partial u_x}{\partial x} \cos^2 \phi + \left(\frac{\partial u_x}{\partial y} + \frac{\partial u_y}{\partial x}\right) \cos \phi \sin \phi + \frac{\partial u_y}{\partial y} \sin^2 \phi = 0 \qquad (2)$$

Equation (2) will hold if the displacements in the x- and y-directions are zero, i.e.,

$$\begin{aligned} u_x &= 0 \\ u_y &= 0 \end{aligned} \qquad (3)$$

For incompressible material, with equation (3), $\partial u_z/\partial z = 0$, and so

$$u_z = \omega(x,y,t) \qquad (4)$$

Here ω is the displacement in z-direction at time t; u_x, u_y, u_z are, respectively, the displacement components in x-, y-, and z-directions. Thus for incompressible material, u_z is uniform through the plate thickness.

The equations (3) and (4) imply shear deformation of the plate, in the sense that plane sections remain plane but do not rotate. This idealized mode of deformation is shown in figure 1.

Then from equations (3) and (4) the velocity components, denoted by v_x, v_y, and v_z, are

$$v_x = 0, \quad v_y = 0, \quad v_z = \partial\omega(x,y,t)/\partial t = v(x,y,t) \tag{5}$$

Equation of Motion

Consider a plate which is struck transversely at the origin at time $t = 0$ by a mass M moving with speed V. The plate, of thickness h, is clamped such that $\omega = 0$ at its edges. The solution to the analogous problem for a beam [3] suggests that the region of the plate bounded by an outwardly propagating wave (curve C, shown in figure 1) moves as a rigid body and the region outside C is at rest. It will be assumed that the wave front remains concentric with the impact point at the center. It is assumed that the impact force is resisted by the dynamic transverse shear stress in the propagating wave C of radius r. The radius of the wave C, at any time t during the impact event, will vary in such a way that dynamic shear stresses on the circumference of this wave balance the impact force at that moment. The equation of motion of the plate inside the wave front can be described by the following expression:

$$(M + m_r)\dot{v} = -2\pi r h S_d \tag{6a}$$

where M is the projectile mass and m_r is the mass of the region of the plate bounded by the wave front of radius r, which can be expressed by the following expression:

$$m_r = \pi r^2 h \rho \tag{6b}$$

By substitution of m_r from equation (6b), the equation (6a) can be rewritten in the following form:

$$(M + \pi r^2 h\rho)\dot{v} = -2\pi rhS_d \tag{6c}$$

where S_d is yield shear stress resultant on the boundary of the curve C. If shear deformations are assumed to be elastic-plastic, the resultant yield shear stress, S_d, will be expressed by the following form:

$$S_d = S_o + G\bar{\nu}^n \tag{7}$$

Where S_o is elastic shear stress, G is the tangential modulus of a strain hardening material (will be taken equal to transverse shear modulus), $\bar{\nu}$ is an equivalent strain on the boundary of the propagating wave front C, and n is strain-hardening exponent of the material.

Considering the dynamic jump condition and discontinuity along the curve C, the second term in equation (7) takes the following form [2] for linear strain-hardening materials (n = 1):

$$G\bar{\nu}^n = \rho C_t v \tag{8}$$

where C_t is equal to $\sqrt{G/\rho}$, known as transverse wave velocity. In case of T300/5208 graphite-epoxy laminates, elastic yield stress will be taken equal to the interlaminar shear stress, S_i. Taking $S_o = S_i$ and substituting the value $G\bar{\nu}^n$ from equation (8), the equation (6) becomes

$$(M + \pi r^2 h\rho)\dot{v} = -2\pi rh(S_i + \rho C_t v) \tag{9}$$

To solve equation (9) we rewrite, after algebraic simplifications, as

$$\frac{d}{dt}[(M + \pi r^2 h\rho)v] = -2\pi rhS_i \tag{10}$$

The operator d/dt can be written in the following form:

$$\frac{d}{dt} = \frac{dr}{dt} \cdot \frac{d}{dr} = C_t \frac{d}{dr}, \quad \text{where} \quad C_t = \frac{dr}{dt} \tag{11}$$

Now, let

$$A = (M + \pi r^2 h\rho)v \tag{12}$$

and

$$B = M + \pi r^2 h\rho$$

Using the relations from equations (11) and (12), the equation (10) is expressed below:

$$C_t \frac{dA}{dr} = - \frac{S_i}{\rho} \frac{dB}{dr} \tag{13}$$

Integration of equation (13) yields

$$C_t A = - \frac{S}{\rho} B + A' \tag{14}$$

where A' is constant of integration. Putting the initial condition, that $r = 0$ at $v = V$, in equation (14) gives the value of the constant of integration, A',

$$A' = M(S_i/\rho + VC_t) \tag{15}$$

Substitution of A' from equation (15) and A and B from equation (12) in equation (13) gives

$$C_t(M + \pi r^2 h\rho)v + \frac{S_i}{\rho} (M + \pi r^2 h\rho) = M\left(\frac{S_i}{\rho} + C_t V\right) \tag{16}$$

Setting the boundary condition that $r = a$ when $v = 0$ in equation (16) gives the radius, a, of the transversely propagating wave front. Equation (16) becomes

$$a = \sqrt{\frac{MC_t V}{\pi h S_i}} \tag{17}$$

Equation (17) gives the radius of the propagating wave front at maximum deflection, which shall be called the radius of the impact affected zone. The mass of the transversely propagating region of the plate, m, during impact is given by

$$m = \pi a^2 h \rho \tag{18}$$

Using the above concepts, it is possible to write the equation of motion during plate rebound. During rebound, it will be assumed that the deformations are elastic, and the resultant yield shear stress will be taken equal to the interlaminar shear stress of the laminate. Thus $S_d = S_i$ and $v = v_r$ in equation (6) gives the equation of motion of the plate during rebound event.

$$(M + \pi r^2 h \rho)\dot{v}_r = -2\pi r h S_i \tag{19}$$

where the suffix r represents the rebound event. Substituting the operator d/dt from equation (11) into equation (19) gives

$$\frac{dv_r}{dr} = -\frac{2\pi h S_i}{C_t} \frac{r}{M + \pi r^2 h \rho} \tag{20}$$

Integration of equation (20) with respect to r gives

$$v_r = -\frac{S_i}{\rho C_t} \log (M + \pi r^2 h \rho) + B' \tag{21}$$

where B' is constant of integration. Setting the initial conditions at the start of rebound event, $v_r = 0$ at $r = a$, gives the constant B',

$$B' = \frac{S_i}{\rho C_t} \log (M + \pi a^2 h\rho) \tag{22}$$

Putting the expression for B' from equation (22) into equation (21) we get

$$v_r = \frac{S_i}{\rho C_t} \log \left(\frac{M + \pi a^2 h\rho}{M + \pi r^2 h\rho} \right) \tag{23}$$

Immediately after detachment, assuming that no mass of the plate vibrates after rebound, $r = 0$, the expression (23) becomes:

$$v_r = \frac{S_i}{\rho C_t} \log \left(1 + \frac{\pi a^2 h\rho}{M} \right) \tag{23a}$$

From equations (17) and (18) it is evident that the mass of the propagating region is proportional to the impact velocity. The combined impact velocity of the target and projectile can be taken equal to M/M' times V where M' is the sum of the projectile mass and the mass of the impact affected zone of the target. The substitution of V by VM/M' in equation (17) and $v_r = -eV$ in equation (23a) gives the relation for the coefficient of restitution, e, by equation (24):

$$e = \frac{-S_i}{\rho V C_t} \log \left(1 + \frac{M}{M'} \frac{\rho C_v V_o}{S_i} \right) \tag{24}$$

Now it is possible to calculate the total energy absorbed by the target, I_a, from equation (1), i.e., $I_a = I(1 - e^2)$, where I is the maximum kinetic energy of the impactor. For a minimum amount of kinetic energy being absorbed by the target, a maximum amount of kinetic energy should be taken away by the impactor during its rebound; this is obtained by maximizing the coefficient of restitution.

Analytical Results

Figure 2 shows the variation of the radius of the impact affected zone, a, with the impact velocity as calculated from equation (17). The value of a is increasing with increase in velocity V . The effect of change in shear modulus, interlaminar shear strength, density of the composite laminate are computed from equation (17) and is shown in figures 3-5. Decrease in transverse shear modulus G of the laminate decreases the radius of the impact affected zone; while the increase in interlaminar shear strength, mass density and thickness of the laminate lowers it. Increases in mass of the impactor and impact velocity cause increase in the radius of this zone as can be seen from equation (17).

The variation of coefficient of restitution with impact velocity is shown in figure 6 as calculated from equation (24). The value of coefficient of restitution is found to decrease with increase in impact velocity. Figures 7-9 show how the shear modulus, interlaminar shear strength and density affect the relation between the impact velocity, V , and the coefficient of restitution, e. Decrease in shear modulus and density are found to increase the coefficient of restitution, but an increase in interlaminar shear strength decreases it. Thus, in order to have a low value of I_a, we should have a high value of interlaminar shear strength and a low value of shear modulus of the laminate. Also, an increase in interlaminar shear strength and decrease in shear modulus lowers the radius of the impact affected zone.

Comparison with Test Results

In order to compare the predictions of the coefficient of restitution, two types of impact tests were conducted:

(1) Free Drop Tests:

Rectangular panels, clamped to provide a free impact area of 90 mm × 150 mm were impacted transversely by free drops of a one-inch diameter steel ball from different heights. The bolts were torqued uniformly to keep mounting conditions uniform. The free-drop impact setup is shown in figure 10. The impact-energy and rebound energy were obtained from the measurements of drop height and rebound height of the ball. Table I lists the impact test data from drop tests.

(2) Instrumented Cantilever Impact Tests:

A one-inch steel ball, with an accelerometer on top, was fixed on the free end of a fiberglass cantilever rod, figure 11. In these tests, circular clamped plates of 50 mm and 90 mm diameter were used. During an impact event, the electric signals from the accelerometer were first processed through a digital data-acquisition system, and then through a computer and placed onto cassette tapes to allow direct acceleration-time data plotting. Double integration of the test data provided velocity-time and displacement-time data. Typical variation of acceleration, velocity and displacement with time is shown in figure 12. Table II gives only the data on impact and rebound velocity because the analysis of impact force and deflection is not within the scope of this report.

The experimental values of the coefficient of restitution from both types of test are plotted in figure 13. The line in figure 13 gives the prediction of the variation of coefficient of restitution with velocity of impact. All the test values are found to lie within a reasonable range of the predicted curve. Thus, this analysis provides a reasonable prediction for the coefficient of restitution over the velocities of impact from 0 to 6 m/sec.

DISCUSSION

The main concept of the approach to the dynamics of transverse loading of plates in this paper is the assumption of inextensibility in the fiber direction and incompressibility in the transverse direction. During loading of the impact event, the resultant shear stress around the circumference of the propogating zone is assumed to be the sum of shear yield stress and the plastic shear stress; whereas during unloading part of the event, the deformations are assumed to be elastic and the resultant shear force around the circumference of the propagating zone is the shear yield stress.

In view of the idealizations made in the presented model, it is interesting to examine the qualitative output of the model. The simple theory provides us the kinetics of impact leading to a mathematical model to evaluate the coefficient of restitution and the impact-affected zone around the point of impact. From equation (16) we see that area of the impact-affected zone is proportional to the impactor's momentum and square root of the transverse shear modulus, G, and inversely proportional to the interlaminar yield shear stress, S_i. Thus small G and large S_i lead to absorption of the kinetic energy of the impactor over a small area of the plate. Also low values of G and large values of S_i (equation (22)) lead to higher values of coefficient of restitution. High values of coefficient of restitution lead to low absorption of kinetic energy. Thus in order to have the lowest value of the kinetic energy absorbed by the target (which means more nearly elastic impact) all the deformations must occur at the point of impact. Such a case corresponds to indentation impact over a plate fixed on rigid elastic plate; this case is outside the scope of the present model.

Comparison of experimental values of coefficient of restitution for transverse impacts of 50 mm and 90 mm diameter plates and 90 mm × 150 mm rectangular plates agreed well with the predictions from the present model. It can be concluded that in case of low velocity transverse impacts of thin laminates made of T300/5208, the coefficient of restitution is a material property which depends strongly upon transverse shear modulus, interlaminar shear strength and the density of the laminate.

ACKNOWLEDGEMENTS

The work conducted in this program was supported by the National Aeronautics and Space Administration under Grant No. NAG-I-196 administered by Langley Research Center, Hampton, Virginia.

SYMBOLS

A', B'	Constants of integration
a	Maximum radius of the impact affected region of the plate
C_t	Transverse shear wave velocity
E_f, C_m	Young's modulii of fibers and matrix
G	Transverse shear modulus
h	Thickness of the plate
I	Maximum kinetic energy of the impactor
I_a	Kinetic energy absorbed by the target during impact process
M	Mass of the impactor
M'	Mass of the impactor plus the moving region of the plate, $M + m$
m	Maximum mass of the propagating region of the plate
m_r	Mass of the propagating region of radius r
r	Radius
S_d	Dynamic shear stress
S_i	Interlaminar strength of the plate
S_w	Shear stress on the boundary of the transverse wave
t	Time
u_x, u_y, u_z	Displacement components in x-, y-, z-directions
V	Maximum velocity of the impactor
v_x, v_t, v_z	Velocity components in x-, y-, z-directions
w	Vertical displacement at any x,y,t
ρ	Mass density of the plate
v	Instantaneous velocity during impact sequence
v_r	Instantaneous velocity during rebound sequence

REFERENCES

1. Spencer, A. J. M., Deformations of Fiber-Reinforced Materials, Clarendon Press, Oxford 1972.

2. Shaw, L. and Spencer, A. J. M., "Transverse Impact of Ideal Fiber-Reinforced Rigid-Plastic Plates," Proc. R. Soc. London, A 361, pp. 43-64, 1978.

3. Shaw, L. and Spencer, A. J. M., "Impulsive Loading of Ideal Fiber-Reinforced Rigid-Plastic Beams," Int. J. Solids Struct. 13, pp. 833-844, 1977.

TABLE I

TEST RESULTS OF FREE BALL DROP TESTS

Impactor : 1-inch diameter steel ball
Target : T300/5208 graphite-epoxy $[45/0/-45/90]_s$ laminate
Impact area: Rectangular 90 mm × 150 mm

Impact		Rebound		Coefficient of restitution, e	
Drop height, m	Maximum velocity, m/s	Rebound height, m	Initial velocity, m/s	Test	Computed
0.30	2.43	0.21	-2.03	0.836	0.8355
.60	3.43	.35	-2.62	.764	.7825
.90	4.20	.57	-3.34	.796	.7464
1.20	4.85	.67	-3.62	.747	.7184
1.50	5.43	.87	-4.14	.762	.6951
1.83	5.99	.92	-4.25	.709	.6752

TABLE II

RESULTS OF CANTILEVER IMPACT TESTS

Impactor : 1-inch diameter steel ball
Target : T300/5208 graphite-epoxy $[45/0/-45/90]_s$ laminate
Impact area: Circular 90 mm and 50 mm diameter

D = 90 mm				D = 50 mm			
V_o	V_r	e		V_o	V_r	e	
m/s	m/s	Test	Computed	m/s	m/s	Test	Computed
0.48	-0.460	0.960	0.962	0.40	-0.400	1.0	0.968
.74	-.705	.952	.943	.725	-.674	.930	.944
1.06	-.943	.890	.920	.930	-.825	.887	.929
1.22	-1.146	.939	.909	1.200	-1.140	.950	.911
1.52	-1.368	.900	.890	1.510	-1.332	.876	.891
1.98	-1.665	.841	.861	2.600	-2.189	.842	.826
2.60	-1.926	.741	.825	3.150	-2.598	.825	.796
3.39	-2.779	.820	.784	3.690	-2.911	.789	.770
3.60	-2.898	.805	.774	4.210	-3.200	.760	.750
3.92	-3.136	.800	.761	5.300	-3.885	.733	.700
4.98	-3.790	.761	.713				
5.47	-3.993	.730	.693				
6.12	-4.437	.725	.673				

V_o, Impact velocity
V_r, Rebound velocity
e, Coefficient of restitution

Caption

1. Idealized dynamic behavior of the laminate.
2. Variation of impact affected zone size with impact velocity.
3. Effect of shear modulus on the size of impact affected zone.
4. Effect of interlaminar shear strength on impact affected zone size.
5. Effect of composite's mass density on impact affected zone size.
6. Variation of coefficient of restitution (C.O.R.) with impact velocity.
7. Effect of shear modulus on coefficient of restitution.
8. Effect of interlaminar shear strength on coefficient of restitution.
9. Effect of composites mass density on coefficient of restitution.
10. Test set-up for free ball drop impact tests.
11. Test set-up for cantilever type instrumented impact tests.
12. Variation of impact force, velocity and deflection with time.
13. Comparison of predicted and test values of coefficient of restitution.

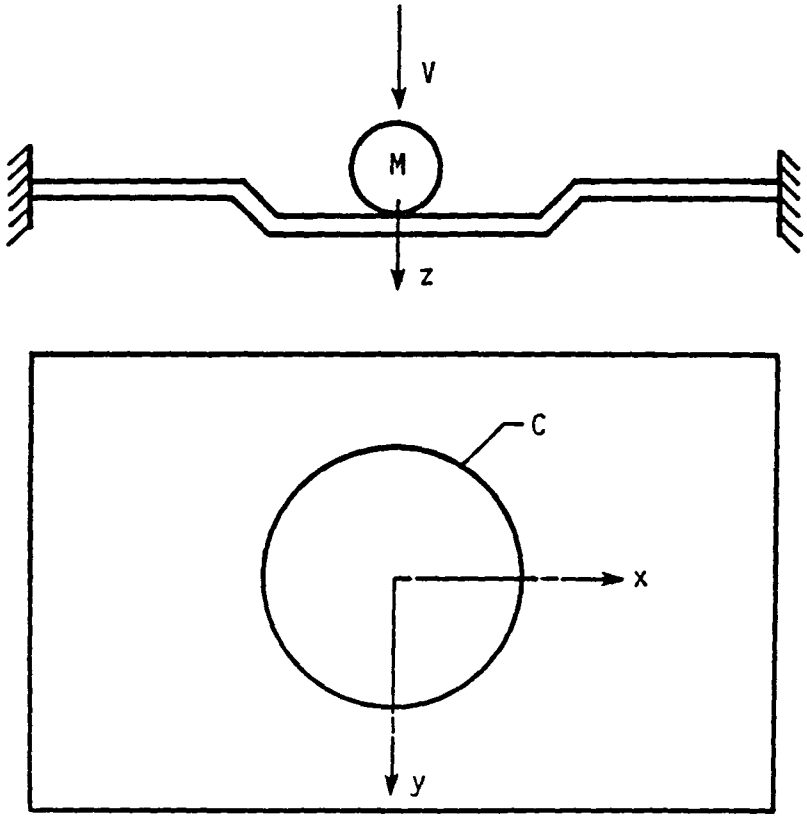

1. Idealized dynamic behavior of the laminate.

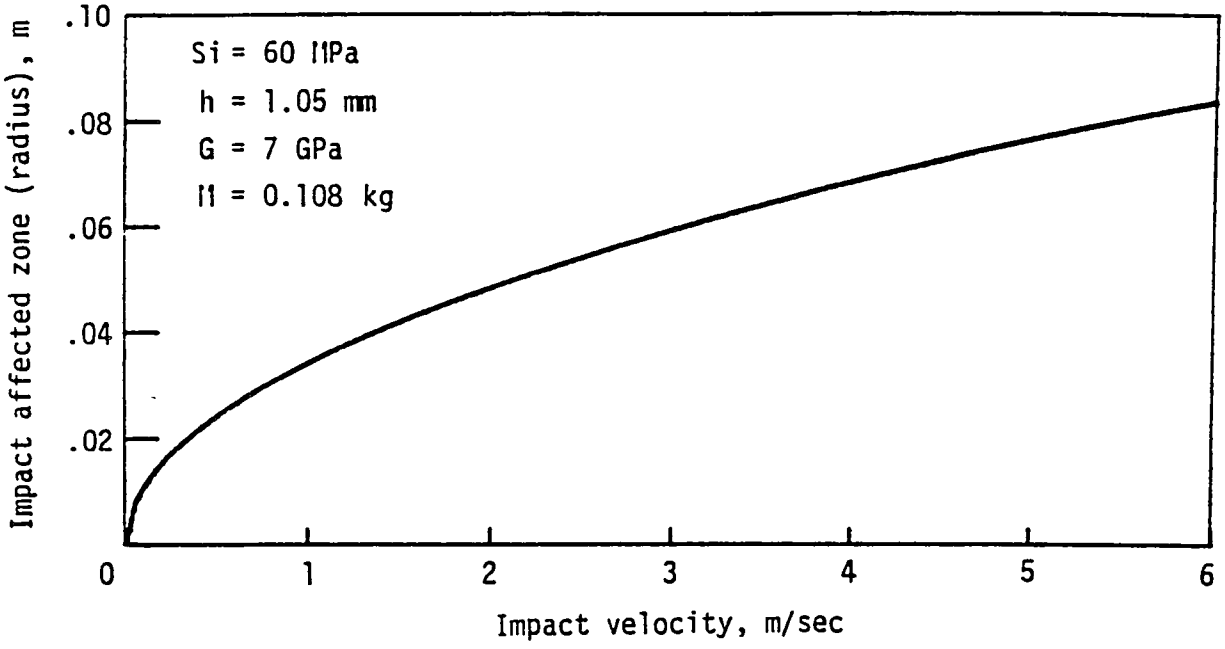

2. Variation of impact affected zone size with impact velocity.

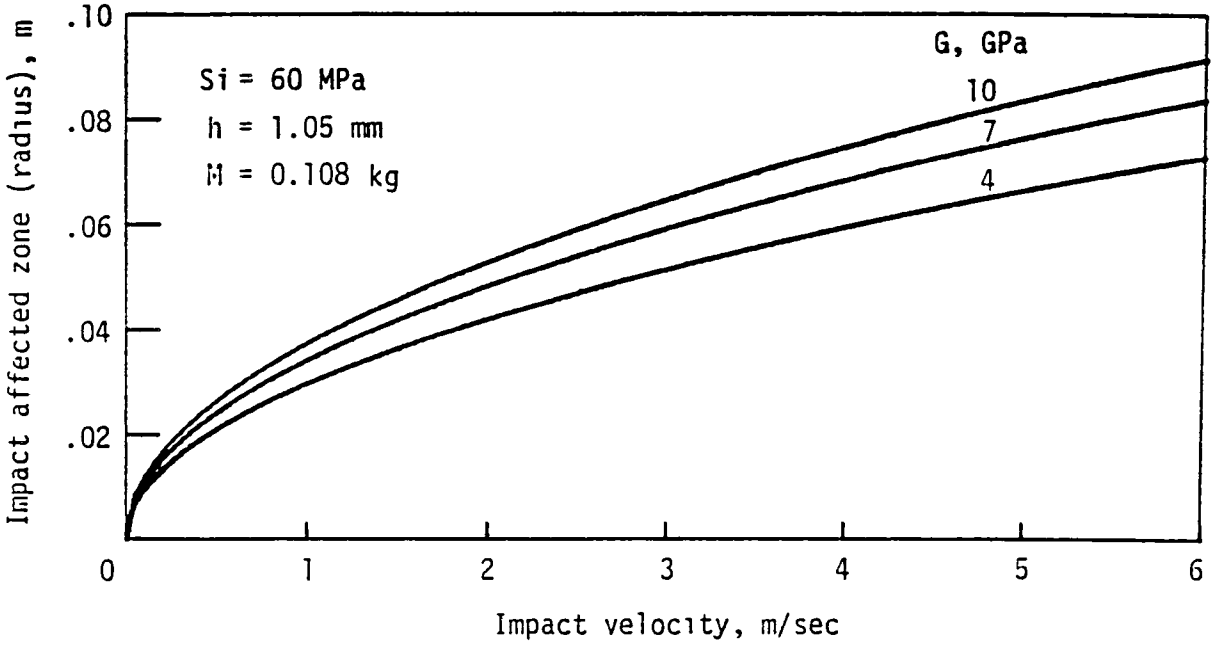

3. Effect of shear modulus on the size of impact affected zone.

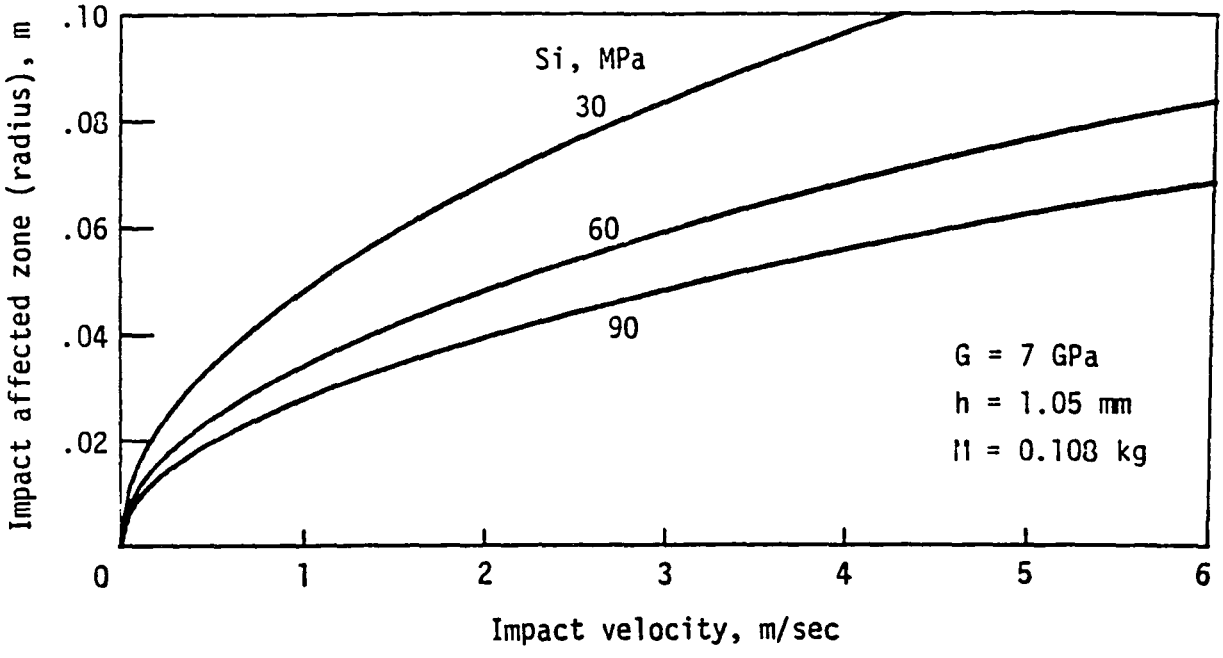

4. Effect of interlaminar shear strength on impact affected zone size.

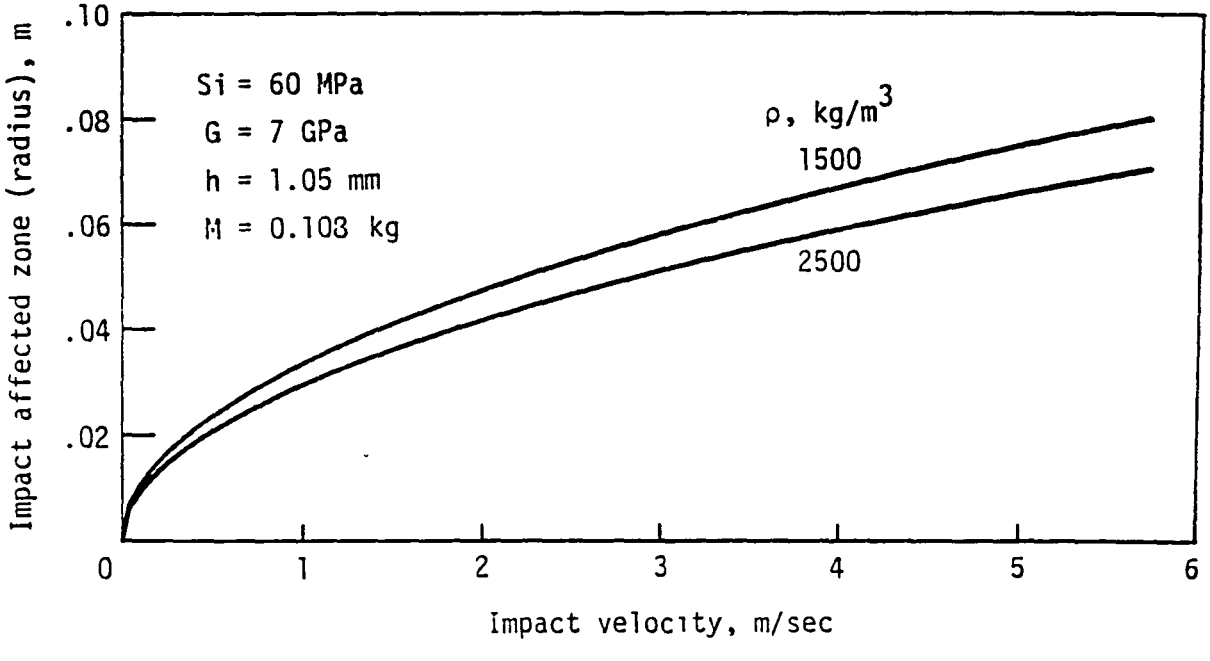

5. Effect of composite's mass density on impact affected zone size.

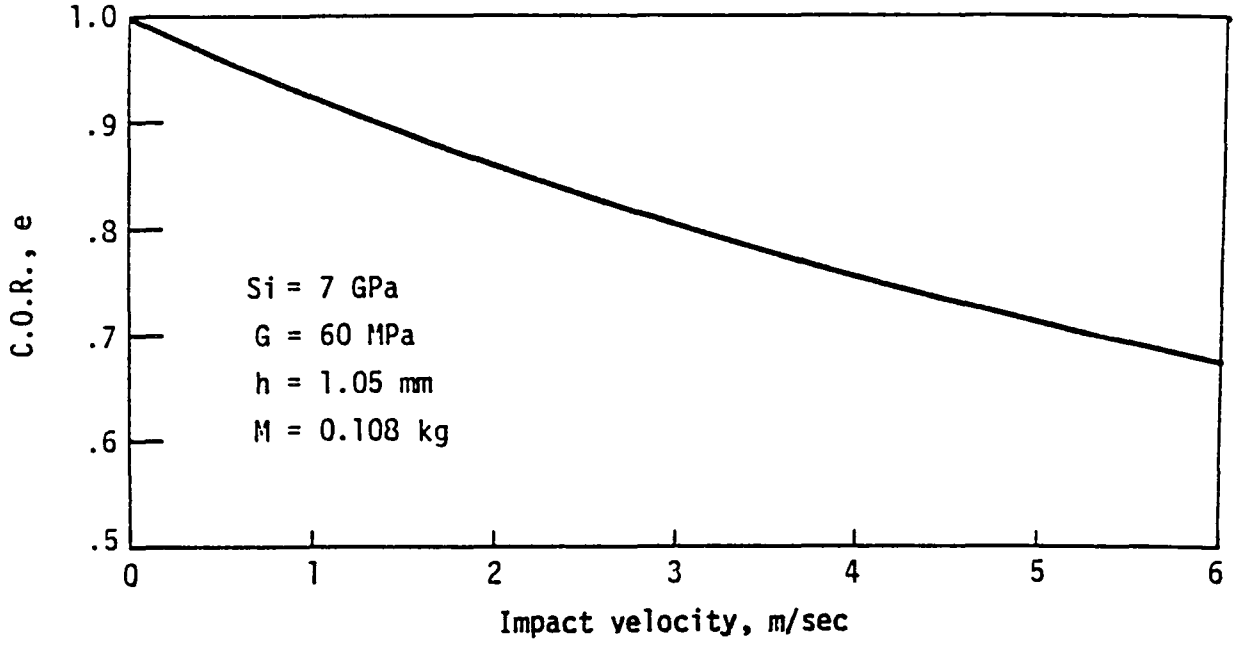

6. Variation of coefficient of restitution (C.O.R.) with impact velocity.

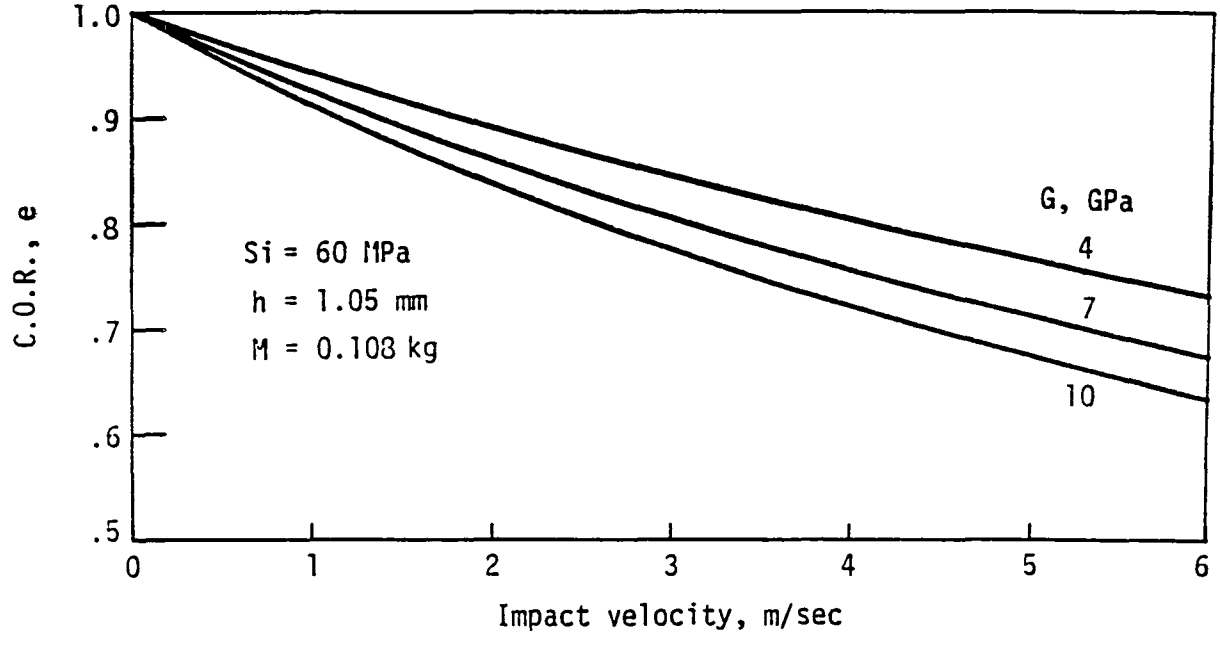

7. Effect of shear modulus on coefficient of restitution.

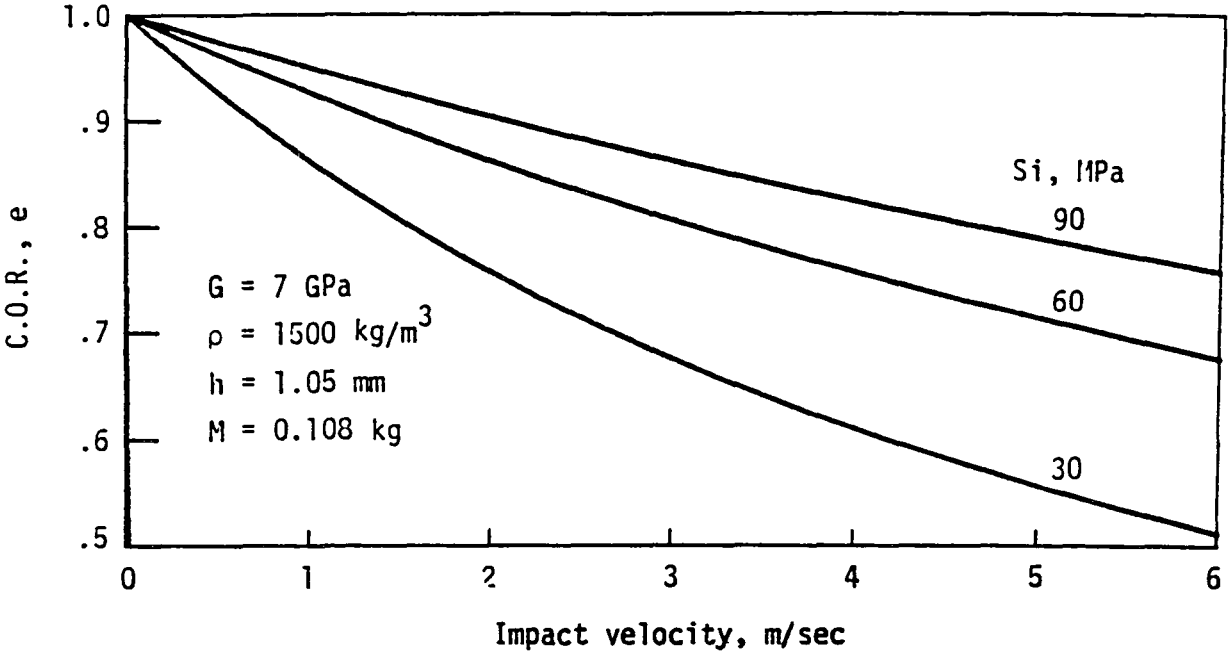

8. Effect of interlaminar shear strength on coefficient of restitution.

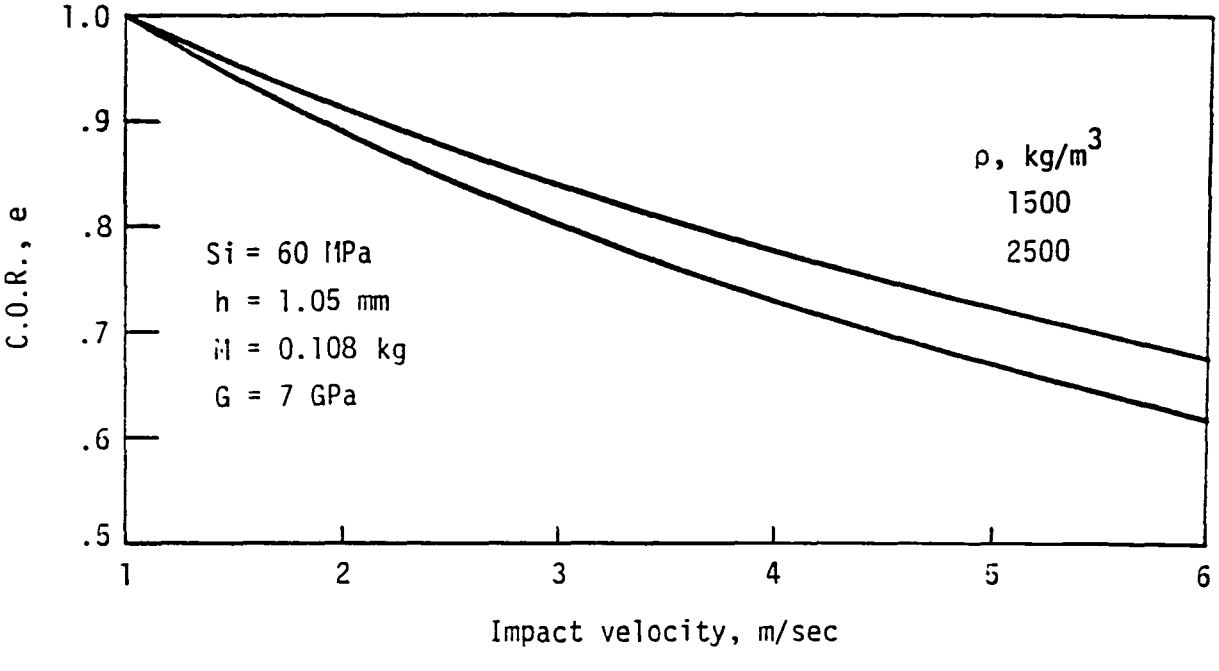

9. Effect of composites mass density on coefficient of restitution.

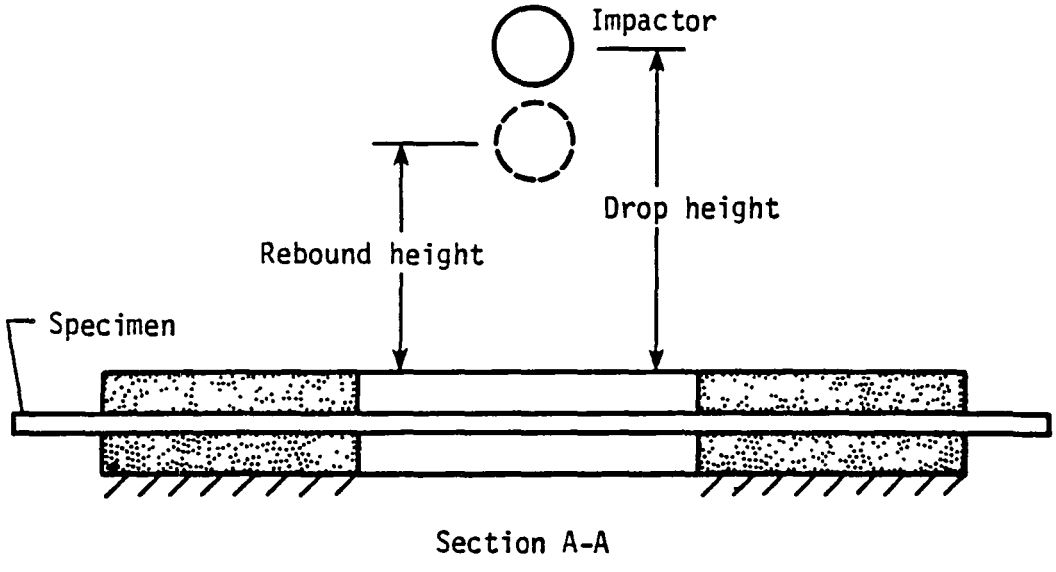

Section A-A

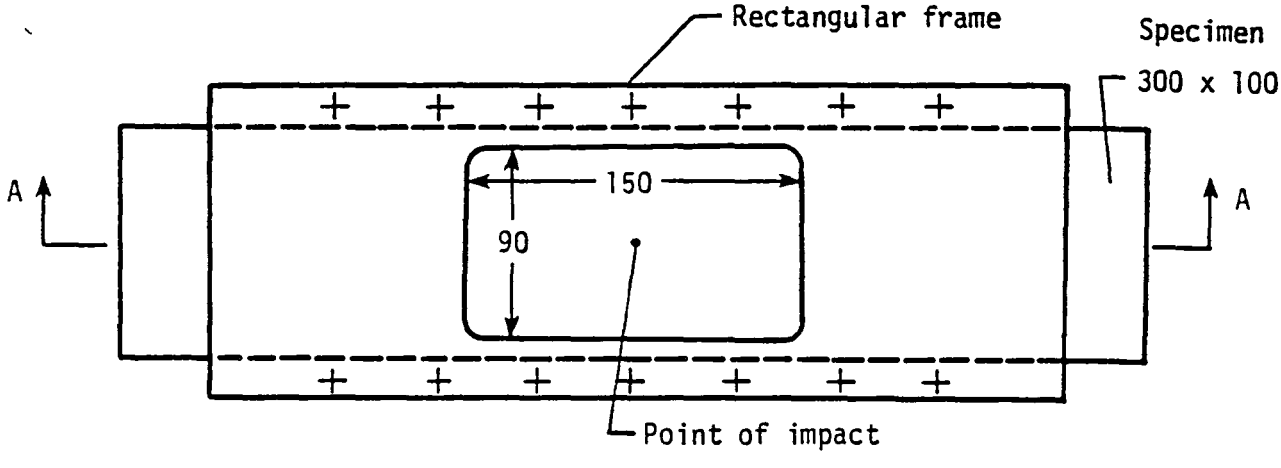

10. Test set-up for free ball drop impact tests.

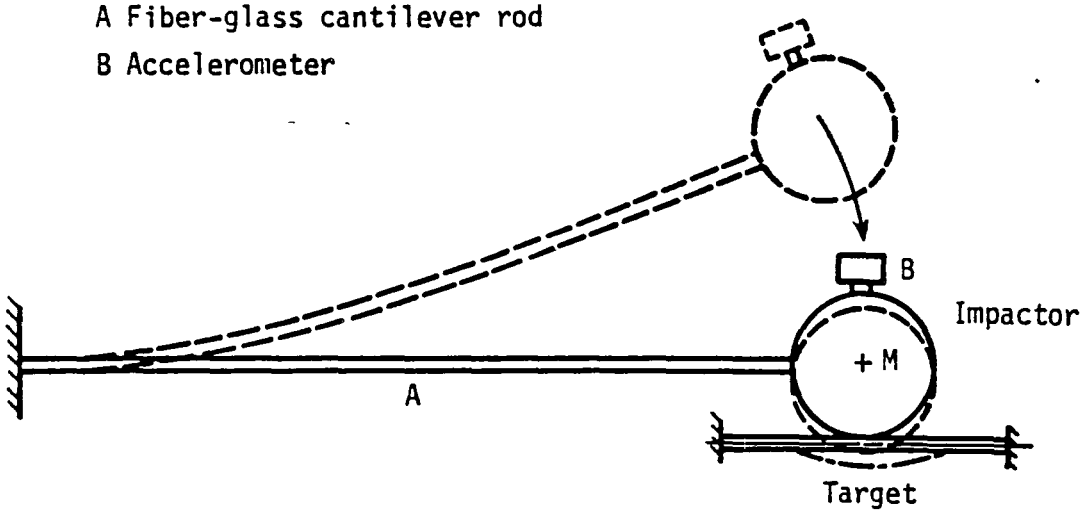

11. Test set-up for cantilever type instrumented impact tests.

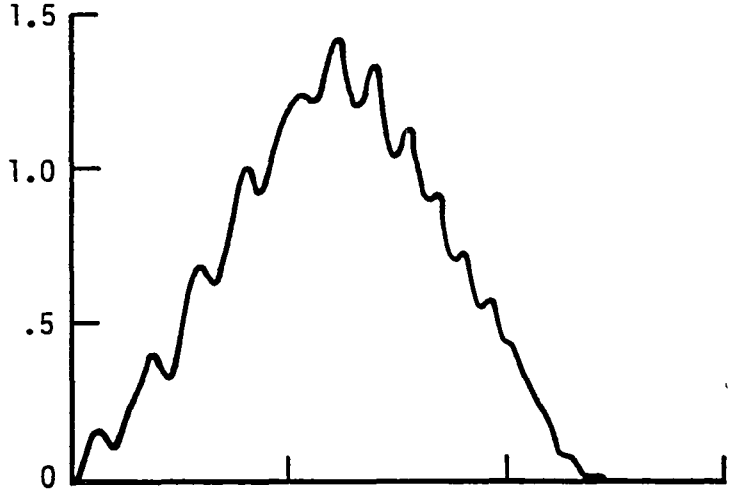

T300/5208
[45, 0, -45, 90] s
Plate dia = 50 mm
Plate thickness = 1.05 mm
Impactors mass = .108 kg
Impact velocity = 3.6 m/sec

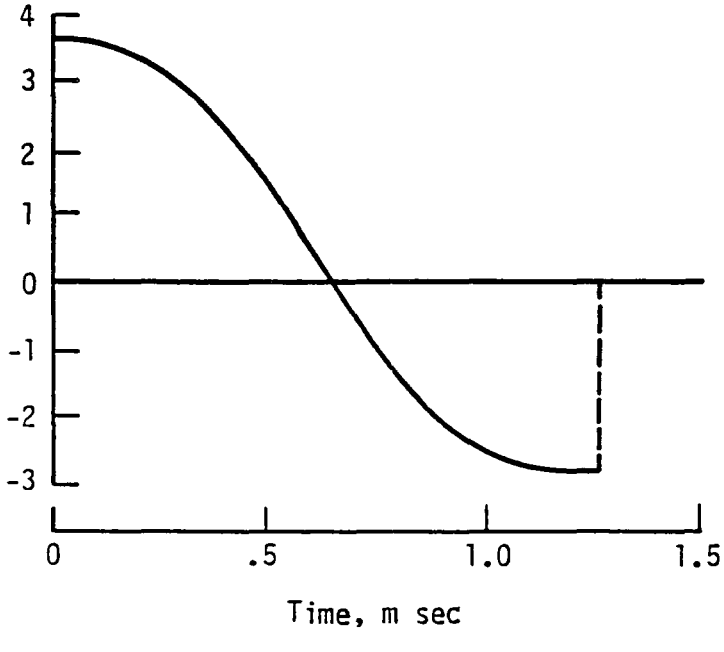

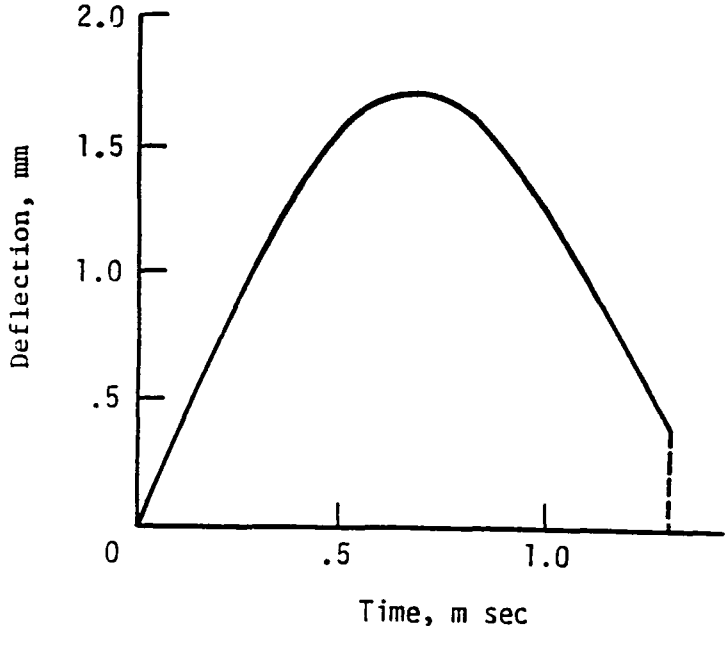

12. Variation of impact force, velocity and deflection with time.

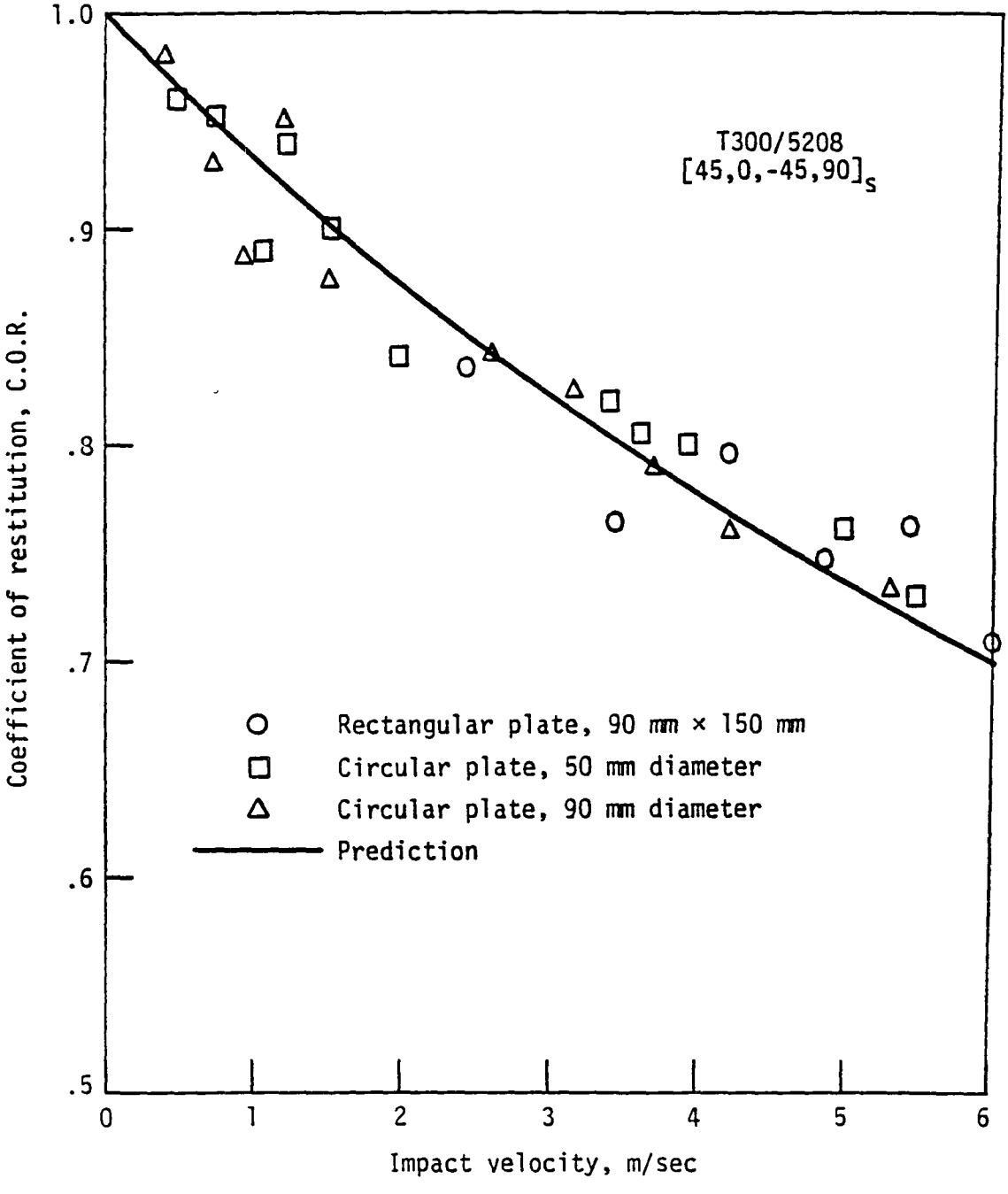

13. Comparison of predicted and test values of coefficient of restitution.

APPENDIX B

Relationship Between Phase Difference and Coefficient of Restitution During Low Velocity Foreign Object Transverse Damage of Composite Plates

K. M. Lal*
NASA Langley Research Center
Hampton, Virginia

Abstract:

This work discusses a model to correlate the coefficient of restitution, of low velocity transverse impacts of graphite-epoxy laminates, with the residual deformation or central deflection at the end of the impact event. It is assumed that the energy absorbed by the target can be calibrated in terms of residual deflection, and thereby in terms of phase difference between the occurrence of impact force and central deflection to their maximas. Analysis was modeled on the basis of the experience from impact tests.

Predictions are compared with the test results of impacted circular and flat plates. Experimentally measured values of coefficient of restitution and phase difference agreed well with the predicted relationship between them.

*Also, Research Associate Professor of Mechanical Engineering and Mechanics at Old Dominion University, Norfolk, Virginia.

During the last decade, significant progress has been made in developing advanced composites possessing high strength, high modulus, and low density, and in understanding their behavior under certain types of loading. As a result, composites such as graphite-epoxy and boron epoxy have been successfully employed as structural materials in aircraft, missiles, and space vehicles, and have satisfactorily demonstrated their performance through extensive ground testing and in flight.

Despite the tremendous advantages that advanced composites have over metals in applications requiring high strength, high stiffness, and low weight, in applications where impact by foreign objects is a design consideration, the advantages inherent in the composites are overshadowed by their poor response to impact loading. Aircrafts, while in service, may be subjected to impacts from hails and bird strikes in the air, runway debris, and even ground service equipment. Such impacts can reduce the strength of the structure.

Literature survey [1] of low velocity foreign object damage to composites, in particular the thin plates of graphite-epoxy, has revealed that the following mechanisms may be expected to operate during the impact event:

(1) Pullout

(2) Debonding

(3) Post debonding friction work

(4) Surface energy

It should be emphasized that it is not necessary that all of the above four mechanisms to operate simultaneously for a given fiber-matrix system. As a result of the above mechanisms, the energy absorbed by the target during impact can be related by the coefficient of restitution [2] such that

$$I_{abs} = I(1 - e^2) \tag{1}$$

where I is impact energy and e is coefficient of restitution of the target. In this work, an attempt is made to correlate the factor e with the phase difference between the maximum impact force and central deflection as seen in the tests.

Tests

In order to understand the impact mechanism of composite plates, few impact tests simulating the low velocity impact conditions were performed. Specimens were of circular plates of 50 mm and 100 mm diameter with clamped boundary. 8-ply and 16-ply plates were tested. Ply orientation, respectively, for 8 -ply and 16-ply plates were $[45,0,-45,90]_s$ and $[45_2,0_2,-45_2,90_2]_s$. Impact was given by an instrumented impactor fixed on the free end of the cantilever, Fig. 1. During an impact event, the electrical signals from the accelerometer (clamped on the top of the impactor) were first processed through a digital data acquisition system, and then through a computer and placed onto cassette tapes to allow direct acceleration-time data plotting. Double integration of the test data provided respectively the velocity-time and displacement data. Typical variation of impact force and displacement with time is shown in Fig. 2. It can be seen that the variation of force looks like sinusoidal, it is zero at the beginning and at the end of the impact event, and that it is maximum at approximately half of the impact duration. The variation of central displacement is also sinusoidal with a phase lag with the impact force. The deflection was zero at the beginning of the impact, reaches to its maximum after the force reaches its maximum value, and there is some residual deflection at the end of the impact event. Amount of residual deflection was increasing with severeness of the impact. This behavior is described that the applied load and resultant deflection are out of phase.

As a result of this phase difference, there is internal friction absorbing energy during the impact event [3]. Obviously, there may be external frictional effects such as air damping, but in present discussions we shall assume these to be negligible and that all damping is internal.

Based on the experience from actual impact test behavior, the variation of impact force and central deflection with time during an impact event are modeled in the next section.

Analysis

The amount of damping or the magnitude of internal friction may be measured in a number of ways, one such being the phase angle ϕ.

Consider the load applied during the impact event has the form

$$P(t) = P_o \sin \frac{\pi}{T} t \tag{2}$$

where $P(t)$ is the load at any time t, T is impact duration, and P_o is maximum load during impact. The load will produce a periodic displacement, $D(t)$ at the point of impact, such that

$$D(t) = D_o \sin\left(\frac{\pi - \phi}{T}\right)t \tag{3}$$

where $D(t)$ is the displacement at time t, D_o is maximum deflection, and ϕ is a parameter for phase difference angle. Putting $t = T$ in equation (3) gives the residual deflection, D_r, at the end of the impact event:

$$D_r = D_o \sin \phi T$$

or

$$\phi T = \sin^{-1}(D_r/D_o) \tag{4}$$

Here ϕT is the measure of phase difference, between the maximum load and maximum deflection, in radians.

The work done or the energy absorbed by the target during impact event is

$$I_{abs} = \int_0^T P(t)\, d(D(t))\, dt \tag{5}$$

Substitution of $P(t)$ and $D(t)$, respectively, from equations (2) and (3) and integrating from zero to T gives

$$I_{abs} = \frac{P_o D_o (1 - z)}{z(2 - z)} (1 - \cos \pi z) \tag{6}$$

where $z = \phi T/\pi$. The time, t_o, when the central deflection is maximum can be obtained from equation (3)

$$t_o = \frac{1}{2} T/(1 - z) \tag{7}$$

The maximum energy, I, of the target is when the deflection is maximum. This is obtained by integrating the equation (5) from time t = zero to t_o, and is

$$I = \frac{1}{2} P_o D_o (1 - z)\left[\frac{1 - \cos\left(\frac{\pi z}{2(1 - z)}\right)}{z} + \frac{1 - \cos\left(\frac{\pi(2 - z)}{2(1 - z)}\right)}{(2 - z)}\right] \tag{8}$$

The ratio of I_{abs} and I gives the relative damping. The coefficient of restitution, e, can be written in terms of the ratio I_{abs}/I by the following equation:

$$e = \left(1 - \frac{I_{abs}}{I}\right)^{1/2} \tag{9}$$

Substitution of I_{abs} and I, respectively, from equations (6) and (8) into equation (9) gives

$$e = \left\{1 - \frac{2(1 - \cos \pi z)}{(2 - z)\left[1 - \cos\left(\frac{\pi z}{2(1 - z)}\right)\right] + z\left[1 - \cos\left(\frac{\pi(2 - z)}{2(1 - z)}\right)\right]}\right\}^{1/2} \qquad (10)$$

The values of coefficient of restitution, e, were computed from equation (10) and are plotted in Fig. 3 as a function of phase difference. It is interesting to mention that the variation of coefficient of restitution with phase difference is independent of time duration of impact.

Results and Discussions

The impact data obtained from tests are given in Table I. Data are plotted on Fig. 3 to compare the validity of the prediction. The agreement between theory and experiment was found better than could reasonably be expected, in view of very simple nature of the theory.

It is important to mention that the predicted relationship between coefficient of restitution and phase difference agrees well with the results of flat surface impact, as well as of clamped plate impact tests. This suggests that the energy absorbed by plates could be predicted by impact testing the flat surface specimens.

Acknowledgements

The work conducted in this program was supported by the National Aeronautics and Space Administration under Grant No. NAG-I-196 administered by Langley Research Center, Hampton, Virginia.

References

1. "Foreign Objects Damage to Composites," ASTM STP 586, 1974.

2. "Impact. The Theory and Physical Behavior of Colliding Solids", Goldsmith, W., Edward Arnold Publishers, Ltd., London, 1960.

3. "Principles of Mechanical Metallurgy," LeMay, I., Elsevier Publishers, New York, 1981, pp. 143-151.

Table I

Test - Data

Laminate		Phase difference, radians	Coefficient of restitution
No. of plies	Plate-diameter mm		
8	50	.038	.997
		.055	.931
		.089	.887
		.125	.877
		.175	.837
		.175	.810
		.214	.788
		.230	.770
		.286	.760
		.326	.735
16	50	.400	.682
		.771	.401
		.539	.485
		.498	.585

Laminate		Phase difference, radians	Coefficient of restitution
No. of plies	Plate-diameter, mm		
16	75	.638	.436
16	100	1.064	.246
16	Flat surface	.095	.869
		.077	.948
		.181	.807
		.302	.706
		.365	.657
		.426	.600
		.402	.610

CAPTIONS

Fig. 1. Lay-out of the cantilever-type instrumented impactor.

Fig. 2. A typical response of acceleration and deflection obtained from accelerometer.

Fig. 3. Comparison of predicted relationship between phase difference and coefficient of restitution with the test data.

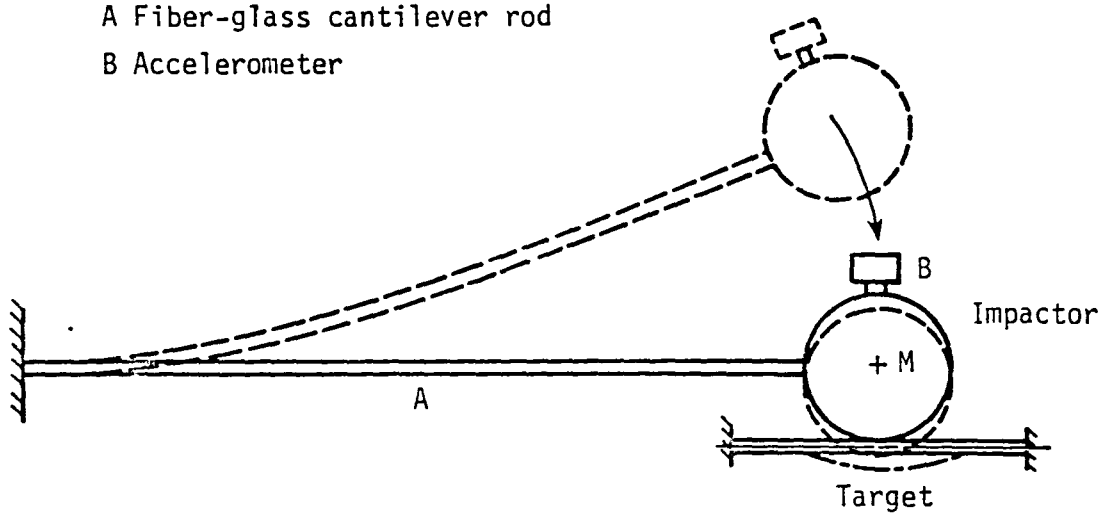

Fig. 1. Lay-out of the cantilever-type instrumented impactor.

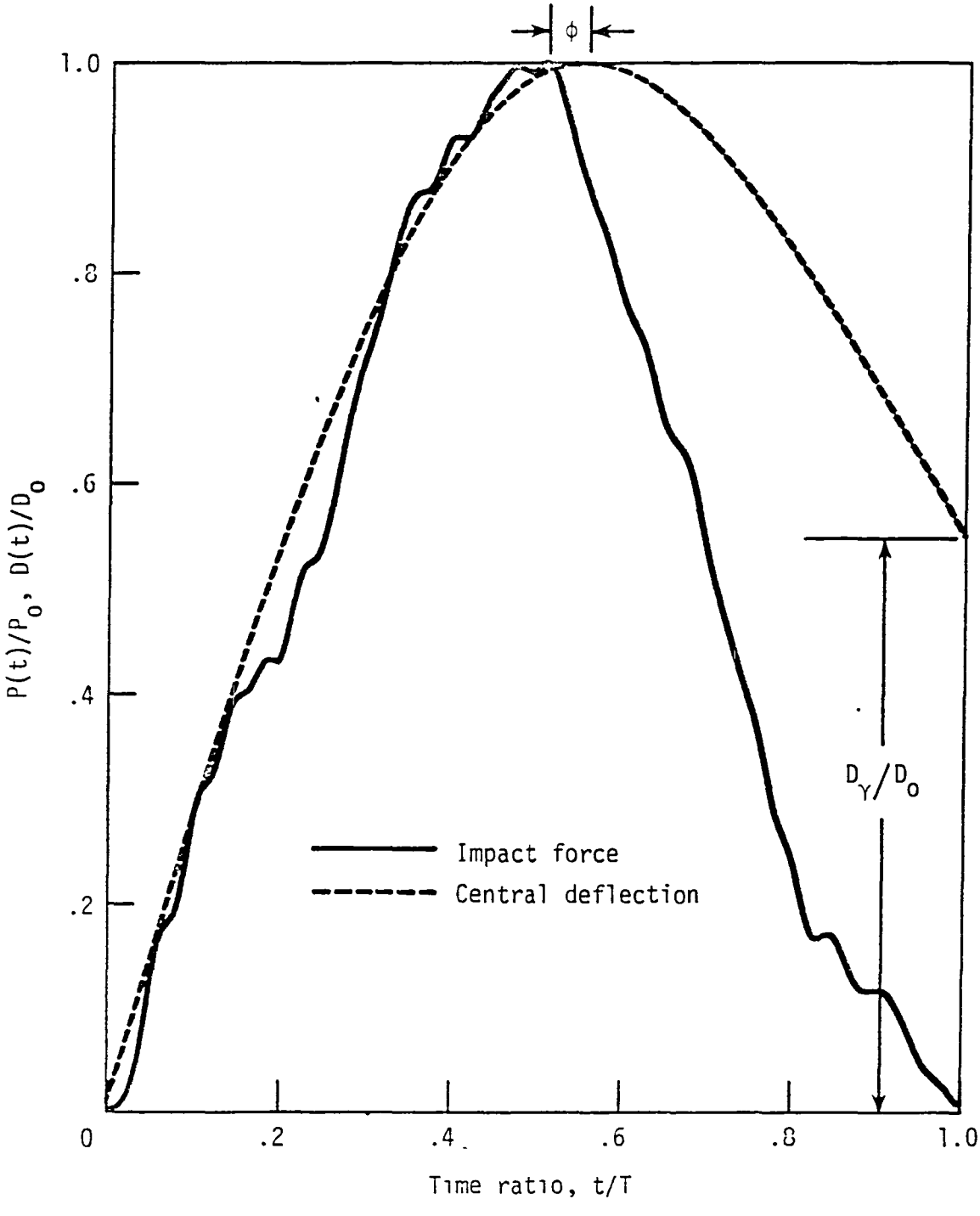

Fig. 2. A typical response of acceleration and deflection obtained from accelerometer.

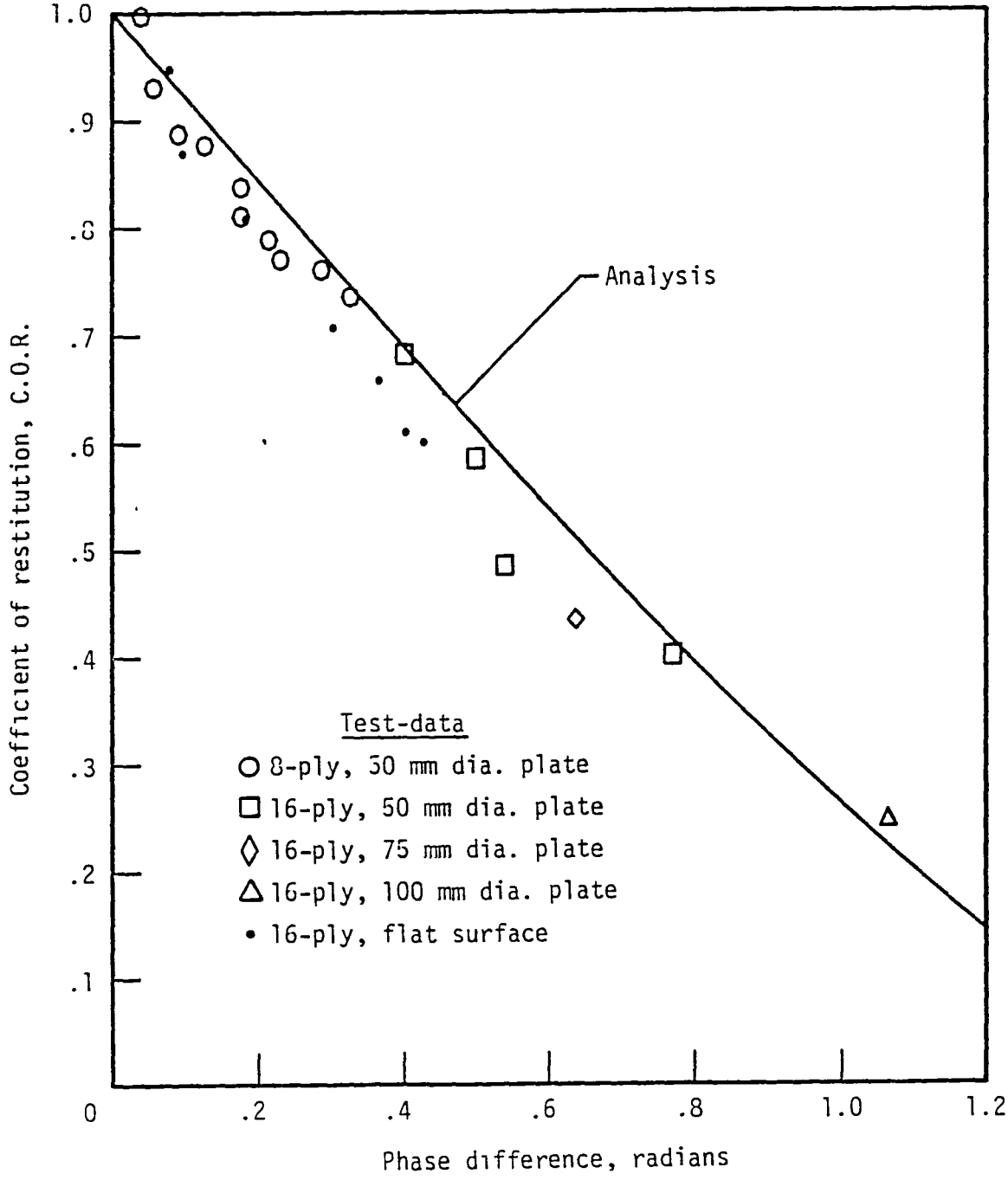

Fig. 3. Comparison of predicted relationship between phase difference and coefficient of restitution with the test data.

End of Document